PHYSICAL REVIEW B **81**, 180405(R) (2010)

Orbital order, stacking defects, and spin fluctuations in the *p*-electron molecular solid RbO_2

E. R. Ylvisaker, R. R. P. Singh, and W. E. Pickett
Department of Physics, University of California, Davis, California 95616, USA
(Received 11 December 2009; revised manuscript received 12 April 2010; published 20 May 2010)

We examine magnon and orbiton behavior in localized O_2 antibonding molecular π^* orbitals using an effective Kugel-Khomskii Hamiltonian derived from a two-band Hubbard model with hopping parameters taken from *ab initio* density-functional calculations. The considerable difference between intraband and interband hoppings leads to a strong coupling between the spin-wave dispersion and the orbital ground state, providing a straightforward way of experimentally determining the orbital ground state from the measured magnon dispersion. The near degeneracy of different orbital ordered states leads to stacking defects which further modulate spin-fluctuation spectra. Proliferation of orbital domains disrupts long-range magnetic order, thus causing a significant reduction in the observed Néel temperature.

DOI: 10.1103/PhysRevB.81.180405 PACS number(s): 71.10.Fd, 75.10.Jm, 75.25.Dk, 75.50.Xx

Correlated systems have generated considerable interest in the literature in recent years. The discovery of high-temperature superconductors and the subsequent development and application of correlated methods such as local-density approximation (LDA) plus intra-atomic Coulomb repusion U (Ref. 1) and dynamical mean field theory (DMFT) (Ref. 2) has led to remarkable success in dealing with strongly correlated systems. At integer filling, strongly correlated systems are typically insulating and often show antiferromagnetic (AFM) behavior arising from exchange or superexchange processes. Such systems include the undoped cuprates, where there is one hole per site that can hop in a square lattice of Cu $d_{x^2-y^2}$ orbitals, and heavy fermion materials such as $CeCuIn_5$ where the Ce $4f$ orbitals weakly couple to the valence states. Multiband correlated systems can also show orbital ordering; the earliest successful application of LDA+U found orbital ordering in the $KCuF_3$ system.[3]

Since correlated behavior is typically the domain of materials with $3d$ and $4f$ orbitals, comparatively little attention has been given to the study of correlated behavior in p-orbital systems. However, local-moment magnetism in $2p$ orbitals has been implicated in several systems, such as at polar oxide vacancies[4] and substitutionals.[5] The occurrence of $2p$-orbital moments at p-type $LaAlO_3/SrTiO_3$ interfaces[6] is still the only viable explanation of the *insulating* character that is observed in these interfaces, where the electron count would suggest metallic interface states. Alkali hyperoxides, to be discussed below, comprise another likely example. Recent calculations[7] suggest that doping of d^0 (no d electrons) magnetic systems can stabilize or even enhance $2p$ magnetic moments in systems such as ZnO nanowires.[7]

Recently, there has been significant interest in studying correlations in solid molecular systems,[8] such as SrN,[9] which consists of Sr octahedra containing either isolated N atoms or N_2 dimers, with calculations predicting that the magnetic moment is strongly confined to the anionic N_2^{2-} dimers. Calculations on the Rb_4O_6 system[10] and Cs_4O_6 (Ref. 11) suggest that these systems would be half-metallic ferromagnets particularly useful for spintronic applications, due to the reduced spin-orbit interaction in p orbitals. However, these calculations were done within weakly correlated density-functional theory (DFT); more recent calculations using LDA+U (Ref. 12) suggest that the valence charge separates to give a mixture of magnetic hyperoxide O_2^- anions and nonmagnetic peroxide O_2^{2-} anions, and an insulating ground state. Early experiments suggest that Rb_4O_6 is conducting based on its black color[13] but recent experiments find insulating character[14] consistent with calculations with include electron correlation effects.[12] In Rb_4O_6, the three different orientations of the O_2 dimers along the principle axes of the crystal give rise to frustration of the magnetic order.

Our interest here is in the alkali hyperoxides, taking RbO_2 as a specific example. Solovyev[15,16] has provided a study of the sister compound KO_2, considering the large spin-orbit coupling (SOC) limit. We present here a complementary viewpoint for RbO_2, with the assumption that the orbital moment is quenched and SOC does not play a significant role. Experimental measurement of the Lande g factor[17] yields values close to 2, suggesting a mostly spin moment, rather than the $g=4/3$ value expected for large spin-orbit coupling, so the neglect of SOC may be reasonable.

The MO_2 systems (M=Li,Na,Rb,Cs) exhibit complex phase diagrams and low-temperature antiferromagnetism.[18] The phase diagrams at low temperature consist of several structural changes which are minor symmetry lowering distortions from the room-temperature (averaged) tetragonal phase which is comparable to a distorted rocksalt structure with O_2^- ions playing the role of the anion, with the molecular axis pointing along the c direction, shown in Fig. 1(b). The Jahn-Teller effect causes the O_2 molecules to tilt away from the tetragonal axis, an effect which is difficult to reproduce in a nonmagnetic LDA calculation. Below 194 K, RbO_2 shows incommensurate superstructure and a mixture of pseudotetragonal, orthorhombic, and monoclinic crystal structures that are all slight distortions of the tetragonal phase.[18]

The standard LDA calculation for RbO_2 produces a half-metallic (ferromagnetic) state in the averaged unit cell,[15] or an antiferromagnetic metal in a Rb_2O_4 supercell, in contrast to experimental reports that MO_2 compounds are insulating.[13] As seen in Fig. 1(a), the $O_2\pi^*$ bands near the Fermi level have a bandwidth of about 1 eV and are well separated from other bands. These bands contain three electrons per O_2^- ion so the occupations of the π_x^* and π_y^* (hereafter $|x\rangle \equiv \pi_x^*$ and $|y\rangle \equiv \pi_y^*$) orbitals are frustrated and likely related to the structural transitions, as well as the Jahn-Teller distortion that tilts the O_2^- ions. Since the relevant bands are

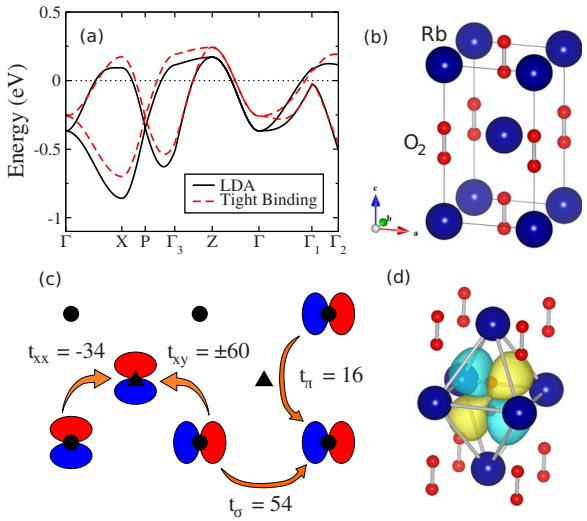

FIG. 1. (Color online) (a) Paramagnetic band plot of RbO_2 showing bands at the Fermi level from both DFT (LDA) and tight binding. The bands are filled such that there is one hole per site. (b) Conventional unit cell of the tetragonal phase of RbO_2. (c) Schematic showing tight-binding hopping parameters in millielectron volt. Circles represent O_2^- anions in a plane perpendicular to the molecular axis and triangles represent O_2^- anions in the nearest planes above or below, Rb not shown. (d) Isosurface of the π_x^* Wannier function in its local environment. (b) and (d) produced with VESTA (Ref. 19).

so narrow and the system is Mott insulating, one might consider the use of the LDA+U method[1] but since the typical implementation of LDA+U in DFT codes uses interactions between onsite atomic orbitals instead of molecular orbitals, a straightforward application of LDA+U fails to produce the correct ground state.[20] The correct ground state can be obtained by manual adjustment of the LDA+U density matrix,[21] although probably not for physically sound reasons.

We used the FPLO code[22] to construct a tight-binding Hamiltonian by projecting Wannier functions using symmetry projected orbitals[23,24] corresponding to the two O_2 molecular π^* orbitals in the primitive cell in a paramagnetic LDA calculation. This allows tight-binding hopping parameters to be calculated directly. We consider only the four most relevant hoppings, two for hopping from corner to the body-centered site $[t_{xx}=\langle \mathbf{0}x|H|\mathbf{R}_1x\rangle$ and $t_{xy}=\langle \mathbf{0}x|H|\mathbf{R}_1y\rangle$, where $\mathbf{R}_1=\frac{1}{2}(a,a,c)]$ and two for the nearest hoppings in the x-y plane $(t_\sigma=\langle \mathbf{0}x|H|\mathbf{R}_{2x}x\rangle$ and $t_\pi=\langle \mathbf{0}x|H|\mathbf{R}_{2y}x\rangle$ with $R_{2x}=a\hat{x}$ and $R_{2y}=a\hat{y}$). The LDA spin-unpolarized band structure and our tight-binding band structure with four parameters are shown in Fig. 1(a). A schematic for the hopping channels used in the tight-binding model is shown in Fig. 1(c) with the numerical values of the hoppings. Note that the largest hopping is t_{xy}, which represents hopping from the corner to the centered site between $|x\rangle$ and $|y\rangle$ orbitals. Hoppings from $|x\rangle$ to $|y\rangle$ between nearest neighbors within the plane are forbidden by symmetry. Each corner site has eight body-centered neighbors with t_{xy} hopping, compared to two each for t_σ and t_π, and since $8|t_{xy}| \gg 2|t_\sigma|+2|t_\pi|$, this would suggest that the strongest AFM coupling is between the body-centered and corner sites, resulting in ferromagnetic planes stacked antiferromagnetically. Previous neutron-diffraction studies[25] on KO_2 show magnetic ordering consistent with this spin ordering.

The noninteracting Hamiltonian is 2×2, with values

$$H^0_{xx} = -8t_{xx}\gamma(\mathbf{k}) - 2t_\sigma \cos k_x - 2t_\pi \cos k_y, \tag{1}$$

$$H^0_{yy} = -8t_{xx}\gamma(\mathbf{k}) - 2t_\pi \cos k_x - 2t_\sigma \cos k_y, \tag{2}$$

$$H^0_{xy} = -4t_{xy}\cos\left(\frac{1}{2}k_z\right)\sin\left(\frac{1}{2}k_x\right)\sin\left(\frac{1}{2}k_y\right), \tag{3}$$

where we define the structure factor between corner and body-centered sites,

$$\gamma(\mathbf{k}) = \cos\left(\frac{1}{2}k_x\right)\cos\left(\frac{1}{2}k_y\right)\cos\left(\frac{1}{2}k_z\right). \tag{4}$$

The interacting Hamiltonian is

$$H = \sum_{i\alpha,j\beta} t_{i\alpha,j\beta} c^\dagger_{i\alpha} c_{j\beta} + \frac{1}{2}U\sum_{i,\alpha,\beta} n_{i\alpha}n_{i\beta}, \tag{5}$$

where i,j run over sites and $\alpha,\beta \in [x,y]$. We apply second-order perturbation theory to H to get an effective Kugel-Khomskii (KK)- (Ref. 26) type Hamiltonian $H_{\mathrm{KK}}=H^{\mathrm{ip}}_{\mathrm{KK}}+H^{\mathrm{sq}}_{\mathrm{KK}}$ for interplanar (ip) and intraplanar (sq) interactions,

$$H^{\mathrm{ip}}_{\mathrm{KK}} = \sum_{\langle i,j\rangle}\left\{\frac{1}{2}(J_{xy}+J_{xx})\left(\mathbf{S}_i\cdot\mathbf{S}_j-\frac{3}{4}\right)+\left[\frac{1}{4}J_{xy}(\tau_i^+\tau_j^+ + \tau_i^-\tau_j^-) + \frac{1}{4}J_{xx}(\tau_i^+\tau_j^- + \tau_i^-\tau_j^+) + \frac{1}{2}(J_{xx}-J_{xy})\tau_i^z\tau_j^z\right]\left(\mathbf{S}_i\cdot\mathbf{S}_j+\frac{1}{4}\right)\right\}, \tag{6}$$

$$H^{\mathrm{sq}}_{\mathrm{KK}} = \sum_{[i,j]}\left\{\frac{1}{4}J_s\left[\mathbf{S}_i\cdot\mathbf{S}_j-\frac{3}{4}+\tau_i^z\tau_j^z\left(\mathbf{S}_i\cdot\mathbf{S}_j+\frac{1}{4}\right)\right]+\frac{1}{4}J_d(\tau_i^z+\tau_j^z)\left(\mathbf{S}_i\cdot\mathbf{S}_j-\frac{1}{4}\right)+J_l(\tau_i^+\tau_j^-+\tau_i^-\tau_j^+)\left(\mathbf{S}_i\cdot\mathbf{S}_j+\frac{1}{4}\right)\right\} \tag{7}$$

in terms of parameters $J_{xy}=4t_{xy}^2/U$, $J_{xx}=4t_{xx}^2/U$, $J_\sigma=4t_\sigma^2/U$, $J_\pi=4t_\pi^2/U$, and $J_s=J_\sigma+J_\pi$ where terms with a single $\tau^\pm$ operators have been neglected. The parameter $J_d=\pm(J_\sigma-J_\pi)$ depends on the direction of the bond between i and j. The τ operators can be represented as Pauli matrices that operate in orbital space. For numerical results, we select $U=3$ eV, which is equivalent to $U_{\mathrm{eff}}=U-J$ for intraorbital U and Hund's exchange J found previously[15] for the $O_2\pi^*$ orbitals in KO_2 via the constrained LDA method.[27] This gives $J_{xx}=1.54$ meV, $J_{xy}=4.8$ meV, $J_\sigma=3.89$ meV, and $J_\pi=0.34$ meV.

Most previous studies[28–31] on the KK Hamiltonian contained only a single parameter t for both intraorbital and interorbital hopping. One of these previous studies[31] concluded that due to unusual symmetries present, the KK Hamiltonian could not describe the observed order and gapped excitations. We consider here a KK-type Hamiltonian constructed via a procedure similar to that of Ref. 32 where the hoppings between orbitals channels are significantly different from hoppings within a channel, as shown in Fig. 1. The broken symmetry of the hoppings in this model should

avoid these difficulties. These hoppings will lead to the orbital ground state having a significant impact on the spin-wave dispersion, which should be measurable in experiment.

To proceed with spin-wave/orbital-wave theory a reference ground state for both the spin and orbital systems must be chosen. From here on, we will consider the electronic structure from the hole perspective so that there is a single hole per site. We restrict our magnetic order to be ferromagnetic within planes and antiferromagnetic stacking of planes.

The ground-state orbital ordering for this model is where antiferro-orbital (AFO) ordering occurs in planes so that a given site with, say, $|x\rangle$ occupied would have first neighbors in the plane with $|y\rangle$ occupied. We refer to this ordering as p type. This ordering frustrates the stacking of the planes so various stackings will be very close in energy and may be degenerate. For these orderings, the spin-wave dispersion $\omega_{\mathbf{k}}^{p}$ and orbital-wave dispersion $\nu_{\mathbf{k}}^{p}$ are given by

$$\omega_{\mathbf{k}}^{p} = \sqrt{(8\bar{J})^2 - [4J_{xy}\gamma_m(\mathbf{k}) + 4J_{xx}\gamma_n(\mathbf{k})]^2}, \tag{8}$$

$$\nu_{\mathbf{k}}^{p} = \sqrt{J_s^2 - \left(\frac{1}{2}J_I\gamma_2(\mathbf{k})\right)^2}, \tag{9}$$

where $\bar{J}=\frac{1}{2}(J_{xy}+J_{xx})$, $J_I=\sqrt{J_\sigma J_\pi}$, and $\gamma_2(\mathbf{k})=\frac{1}{2}(\cos k_x + \cos k_y)$. where the effect of different stackings is contained in the structure factors $\gamma_m(\mathbf{k})$ and $\gamma_n(\mathbf{k})$. First we consider the case of *ABAB* stacking, where any given site has the same orbital occupation as the sites at displacements $(0,0,c)$ and $(0,0,-c)$ from it. This results in structure factors given by

$$\gamma_m(\mathbf{k})^{ABAB} = \cos\left[\frac{1}{2}(k_x+k_y)\right]\cos\left(\frac{1}{2}k_z\right),$$

$$\gamma_n(\mathbf{k})^{ABAB} = \cos\left[\frac{1}{2}(k_x-k_y)\right]\cos\left(\frac{1}{2}k_z\right). \tag{10}$$

An alternate stacking, *ABCD*, where each site has the opposite orbital occupation as the sites above and below in the $\hat{z}$ direction, has structure factors of

$$\gamma_m(\mathbf{k})^{ABCD} = \cos\frac{k_x}{2}\cos\frac{k_y}{2}\cos\frac{k_z}{2} + i\,\sin\frac{k_x}{2}\sin\frac{k_y}{2}\sin\frac{k_z}{2},$$

$$\gamma_n(\mathbf{k})^{ABCD} = \cos\frac{k_x}{2}\cos\frac{k_y}{2}\cos\frac{k_z}{2} - i\,\sin\frac{k_x}{2}\sin\frac{k_y}{2}\sin\frac{k_z}{2}. \tag{11}$$

The dispersions are depicted in Fig. 2(a).

An alternate orbital ordering we consider is where the ordering within planes are ferro-orbital (FO) ordering. This ordering is not stable to orbital fluctuations within our KK model, however it may be stabilized in RbO_2 by effects not considered here, such as the Jahn-Teller distortion that causes the canting of the O_2 molecules. This ordering is of particular interest because if the stacking of planes is AFO, then the corner to body-centered spin exchange is maximized. With this orbital ordering (hereafter referred to as *xy* ordering), the spin sublattices have different dispersions due to the swapping of J_σ and J_π in each plane. The Kugel-Khomskii Hamiltonian yields a spin-wave dispersion of

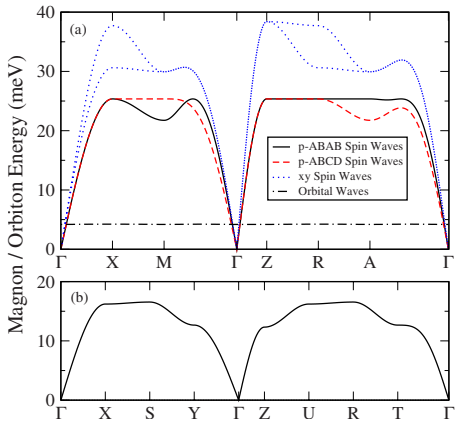

FIG. 2. (Color online) (a) Spin-wave spectrum for RbO_2 for p-type ordering for both stackings as described in text (black solid, *ABAB* stacking and red dashed, *ABCD* stacking), and spin-wave spectrum for *xy* ordering (blue dotted). Also, the nearly dispersionless orbital spectrum is shown for p-type orderings (black dashed-dotted line). (b) Spin-wave spectrum for ferro-orbital ordering, which is orthorhombic symmetry.

$$\omega_{\mathbf{k}}^{xy} = \sqrt{A_m^2 - [8J_{xy}\gamma(\mathbf{k})]^2} \pm A_d \tag{12}$$

with $A_m=8J_{xy}-J_s[2-\cos(k_x)-\cos(k_y)]$ and $A_d=(J_\sigma - J_\pi)[\cos(k_x)-\cos(k_y)]$, and is shown in Fig. 2(a).

Thus far, the orderings considered all preserve tetragonal symmetry but orthorhombic and monoclinic low-temperature phases of RbO_2 exist. The final orbital ordering we consider is FO ordering for every site in the crystal, hereafter called *xx* ordering, which is orthorhombic symmetry. This has spin-wave dispersion $\omega_{\mathbf{k}}^{xx}=\sqrt{A_{\mathbf{k}}^2-B_{\mathbf{k}}^2}$, where $A_{\mathbf{k}}=8J_{xx}+\frac{1}{2}(J_s - J_\sigma\cos k_x - J_\pi\cos k_y)$ and $B_{\mathbf{k}}=8J_{xx}\gamma(\mathbf{k})$. Again, this configuration is not stable with respect to orbital fluctuations but it may be stabilized by effects not considered here. LDA $+U$ calculations of KO_2 suggest this is the case,[33] and spin-wave calculations[15] suggest that this state is at least dynamically stable. The magnon dispersion is shown in Fig. 2(b).

The ground-state energies for these four orbital orderings are listed in Table I, where we find that the *ABAB* stacking of planar orbital ordering is the lowest energy. For an average corner to body-centered spin exchange of $\bar{J}=3.17$ meV (in p-type orderings), high-temperature series expansion[34] would predict $T_N\approx 1.4\bar{J}=51$ K, much higher than the observed $T_N=15$ K. The frustrated exchanges within planes

TABLE I. Energies contributing to the ground-state energy in millielectron volt. E_0 is the classical ground-state energy and $E_S(E_O)$ is the quantum correction from spin (orbital)-wave theory.

	Orbital order			
	xx	*xy*	*p-ABAB*	*p-ABCD*
E_0	−12.680	−12.680	−14.795	−14.795
E_S	−0.411	−3.266	−2.333	−2.288
E_O	0	0	−0.010	−0.010
E_{tot}	−13.091	−15.946	−17.138	−17.093

would reduce this value somewhat but not enough to give a prediction reasonably close to the experimental transition.

As expected, the two stackings examined for the planar orbital ordering are very nearly degenerate, with only quantum fluctuations in the spin waves breaking the degeneracy at this level of approximation. It is rather clear that due to the strong asymmetry between hopping within an orbital channel and hopping between orbital channels, the orbital ground state significantly impacts the spin-wave spectrum and could be inferred from a measurement of the low-temperature magnons. The planar orbital orderings do not significantly impact the spin-wave dispersion so even if the stacking is disordered magnon excitations should be coherent. Energetically, the next state above *p*-type ordering is the *xy* ordering, which is ~ 1.2 meV≈ 14 K higher in energy than *p*-type ordering. Above this temperature, orbital domains should proliferate. The strong modulation of exchange constants at the domain boundaries should nucleate magnetic domains,[35] leading to the low observed Néel temperature of RbO_2 of 15 K. It should be noted that a recent LDA+U study on KO_2 obtained a different ground-state orbital configuration,[21] however the authors did not use a supercell which allowed antiferro-orbital ordering within the planes.

Orbitons are quite difficult to measure experimentally. They do not couple directly to neutrons, the standard measurement technique for magnons. Recently, orbitons have been measured in titanates via x rays[36] but the inference of the orbital dispersion is very indirect. The measured dispersion is negligible, suggesting[36] that x-ray modulate bonds resulting in a much bigger scattering from two orbitons than from single orbitons. It may be that in narrow-band molecular-oxide systems, the x rays will create single orbiton excitations with all bond modulation inside a unit cell. If that is the case, the x-ray-measured dispersion in RbO_2 should be clearly observable, if a similar experiment can be done. Neglected here is the Jahn-Teller effect which rotates the O_2 molecules and breaks the orbital degeneracy, which will select a particular ground-state orbital ordering.

We have examined independent magnon and orbiton excitations in RbO_2 within spin-wave/orbital-wave theory, finding considerable coupling between the easily measured magnon excitations and the difficult to measure orbital ground state. This strong coupling arises from the large anisotropy in the hopping parameters in the $O_2\pi^*$ bands. This indicates that MO_2 materials are attractive for studying the interplay between orbital ordering and *p*-electron magnetism.

E.R.Y. and W.E.P. were supported by DOE SciDAC under Grant No. DE-FC02-06ER25794. The authors would like to thank J. Kuneš, R. T. Scalettar, and C. Felser for stimulating conversation.

[1] V. I. Anisimov, F. Aryasetiawan, and A. I. Lichtenstein, J. Phys.: Condens. Matter **9**, 767 (1997).
[2] A. Georges, G. Kotliar, W. Krauth, and M. J. Rozenberg, Rev. Mod. Phys. **68**, 13 (1996).
[3] J. E. Medvedeva, M. A. Korotin, V. I. Anisimov, and A. J. Freeman, Phys. Rev. B **65**, 172413 (2002).
[4] I. S. Elfimov, S. Yunoki, and G. A. Sawatzky, Phys. Rev. Lett. **89**, 216403 (2002).
[5] V. Pardo and W. E. Pickett, Phys. Rev. B **78**, 134427 (2008).
[6] R. Pentcheva and W. E. Pickett, Phys. Rev. B **74**, 035112 (2006).
[7] H. Peng, H. J. Xiang, S.-H. Wei, S.-S. Li, J.-B. Xia, and J. Li, Phys. Rev. Lett. **102**, 017201 (2009).
[8] O. Volnianska and P. Boguslawski, J. Phys.: Condens. Matter **22**, 073202 (2010).
[9] O. Volnianska and P. Boguslawski, Phys. Rev. B **77**, 220403(R) (2008).
[10] J. J. Attema, G. A. de Wijs, G. R. Blake, and R. A. de Groot, J. Am. Chem. Soc. **127**, 16325 (2005).
[11] J. J. Attema, G. A. de Wijs, and R. A. de Groot, J. Phys.: Condens. Matter **19**, 165203 (2007).
[12] J. Winterlik, G. H. Fecher, C. A. Jenkins, C. Felser, C. Mühle, K. Doll, M. Jansen, L. M. Sandratskii, and J. Kübler, Phys. Rev. Lett. **102**, 016401 (2009).
[13] M. Jansen, R. Hagenmayer, and N. Korber, C. R. Acad. Sci. Paris **2**, 591 (1999).
[14] J. Winterlik *et al.*, Phys. Rev. B **79**, 214410 (2009).
[15] I. V. Solovyev, New J. Phys. **10**, 013035 (2008).
[16] I. V. Solovyev, J. Phys.: Condens. Matter **20**, 293201 (2008).
[17] M. Labhart, D. Raoux, W. Känzig, and M. A. Bösch, Phys. Rev. B **20**, 53 (1979).
[18] M. Rosenfeld, M. Ziegler, and W. Känzig, Helv. Phys. Acta **51**, 298 (1978).
[19] K. Momma and F. Izumi, J. Appl. Crystallogr. **41**, 653 (2008).
[20] J. Winterlik, G. H. Fecher, and C. Felser, J. Am. Chem. Soc. **129**, 6990 (2007).
[21] R. Kováčik and C. Ederer, Phys. Rev. B **80**, 140411(R) (2009).
[22] K. Koepernik and H. Eschrig, Phys. Rev. B **59**, 1743 (1999).
[23] W. Ku, H. Rosner, W. E. Pickett, and R. T. Scalettar, Phys. Rev. Lett. **89**, 167204 (2002).
[24] E. R. Ylvisaker and W. E. Pickett, Phys. Rev. B **74**, 075104 (2006).
[25] H. G. Smith, R. M. Nicklow, L. J. Raubenheimer, and M. K. Wilkinson, J. Appl. Phys. **37**, 1047 (1966).
[26] K. I. Kugel' and D. I. Khomskii, Sov. Phys. Usp. **25**, 231 (1982).
[27] O. Gunnarsson, O. K. Andersen, O. Jepsen, and J. Zaanen, Phys. Rev. B **39**, 1708 (1989).
[28] G. Khaliullin and V. Oudovenko, Phys. Rev. B **56**, R14243 (1997).
[29] L. F. Feiner, A. M. Oles, and J. Zaanen, Phys. Rev. Lett. **78**, 2799 (1997).
[30] A. B. Harris, A. Aharony, O. Entin-Wohlman, I. Y. Korenblit, and T. Yildirim, Phys. Rev. B **69**, 094409 (2004).
[31] A. B. Harris, T. Yildirim, A. Aharony, O. Entin-Wohlman, and I. Y. Korenblit, Phys. Rev. B **69**, 035107 (2004).
[32] R. Schmitz, O. Entin-Wohlman, A. Aharony, A. B. Harris, and E. Müller-Hartmann, Phys. Rev. B **71**, 144412 (2005).
[33] M. Kim, B. H. Kim, H. C. Choi, and B. I. Min, Phys. Rev. B **81**, 100409(R) (2010).
[34] J. Oitmaa and W. Zheng, Phys. Rev. B **69**, 064416 (2004).
[35] I. I. Mazin and M. D. Johannes, Nat. Phys. **5**, 141 (2009).
[36] C. Ulrich *et al.*, Phys. Rev. Lett. **103**, 107205 (2009).